

EUV spectra of Rb-like to Ni-like dysprosium ions in an electron beam ion trap

Deirdre Kilbane¹, Gerald O'Sullivan¹, Yuri A. Podpaly², John D. Gillaspay², Joseph Reader², and Yuri Ralchenko^{2,a}

¹ School of Physics, University College Dublin, Belfield, Dublin 4, Ireland

² National Institute of Standards and Technology, Gaithersburg, Maryland 20899, USA

Received 26 February 2014 / Received in final form 2 May 2014

Published online 12 August 2014 – © EDP Sciences, Società Italiana di Fisica, Springer-Verlag 2014

Abstract. Extreme ultraviolet radiation emitted from highly-charged dysprosium ions was measured at the National Institute of Standards and Technology. The ions were created, trapped, and excited in an electron beam ion trap (EBIT), and the spectra were recorded with a flat-field grazing-incidence spectrometer in the wavelength range 3 nm to 17 nm. Tuning the electron beam energies between 1.2 keV and 2.0 keV resulted in a selection of Rb-like Dy²⁹⁺ to Ni-like Dy³⁸⁺ ions. Identification of strong $n = 4-n = 4$ transitions was achieved by collisional-radiative modeling of the EBIT plasma. A total of 64 spectral lines were recorded, including 54 new identifications.

1 Introduction

Identification of intense sources of extreme ultraviolet (EUV) radiation in the 6.6–6.8 nm wavelength region is crucial to the future of next-generation lithography and a research priority for the semiconductor industry. EUV emission from $4d-4f$ and $4p-4d$ transitions in highly ionized gadolinium and terbium ions in laser produced plasmas have been extensively investigated with a view to optimizing emission at the peak reflectivity of LaN/B and LaN/B₄C multilayer mirrors [1–6]. Strong emission arising from these $n = 4-n = 4$ unresolved transition arrays (UTAs) moves to shorter wavelengths with increasing nuclear charge, Z [7–10]. From Figure 1 of reference [11], it can be inferred that the calculated peak reflectivity of LaN/B₄C mirrors is approximately 70% between 6.6 and 6.8 nm (using measured optical constants [12]). Here we propose to couple the emission from a single narrow strong transition of a highly charged Dy ion with LaN/B₄C multilayer mirrors. This will increase conversion efficiency by significantly reducing band emission and debris, both undesirable properties of current UTA sources such as tin, gadolinium and terbium.

Since the 1980's a large number of measurements of EUV radiation emitted from highly charged dysprosium ions in laser-produced plasmas and tokamak devices have been reported. These include Cu-like [13–19], Zn-like [13,17–21], Ga-like [17,19,21] and Ni-like [22,23] during the investigation of potential X-ray lasers. Seely et al. [16] performed multiconfiguration Dirac-Fock (MCDF) calculations of wavelengths and energy levels of the Cu isoelectronic sequence with the Grant code [24]. Sugar et al. [18] and Kim et al. [25] followed these with

calculations using the MCDF Desclaux code [26] where the latter included quantum-electrodynamic (QED) corrections. Brown et al. performed similar calculations for the Zn isoelectronic sequence using the Hebrew University Lawrence Livermore Atomic Code (HULLAC) [27,28]. Ab initio atomic structure calculations of Ga-like dysprosium using the parametric potential code RELAC, the relativistic version of MAPPAC [29,30] were presented in reference [19]. For Ni-like dysprosium, Scofield and MacGowan [22] carried out relativistic multi-configuration Hartree-Fock calculations, while Daido et al. [23] employed the general purpose relativistic atomic-structure program (GRASP) code [31].

In this work we used the electron beam ion trap (EBIT) at the National Institute of Standards and Technology (NIST) to identify spectral lines in Dy²⁹⁺-Dy³⁸⁺. This is a continuation of a previous series of measurements on $n = 4-n = 4$ EUV transitions in tungsten, hafnium, tantalum, gold, and gadolinium [32–35].

2 Experiment

A detailed description of the NIST EBIT is presented in reference [36]. For the present work, the electron beam energy was varied between 1.20 keV and 2.90 keV, with beam currents in the range of 18.5 mA to 80 mA. A superconducting Helmholtz-pair magnet provided a 2.7 T axial magnetic flux density, which compressed the electron beam to a radius of $\approx 30 \mu\text{m}$, giving a high current density. Dysprosium ions were produced in a metal vapour vacuum arc (MEVVA) [37] ion source and subsequently injected into the EBIT. A vacuum of typically 3.2×10^{-8} Pa was maintained in the EBIT. The trap of depth 220 V was emptied every 10 s to prevent the buildup of contaminating ions.

^a e-mail: Yuri.Ralchenko@nist.gov

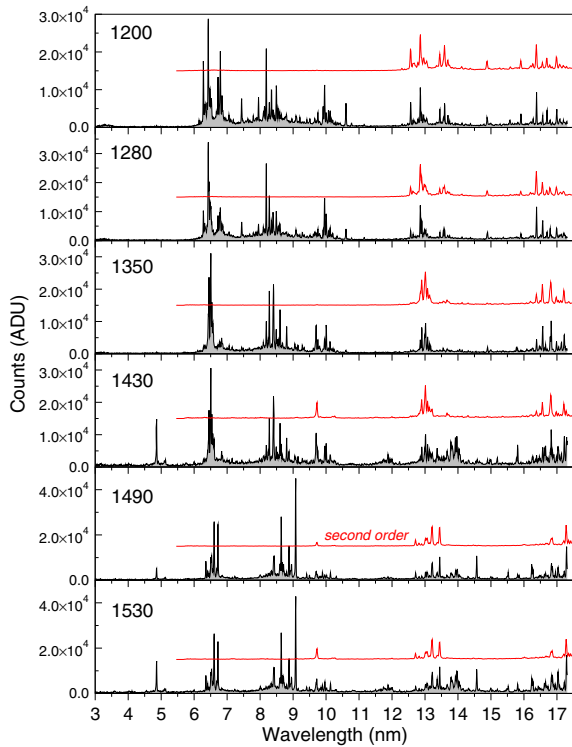


Fig. 1. Experimental spectra of Dy ions. Nominal electron beam energies (in eV) are shown in the upper left corners.

The spectra in the wavelength range 3 nm to 17 nm were recorded with a flat-field grazing-incidence spectrometer [38]. The spectrometer houses a gold-coated-concave variable-spaced reflection grating with groove spacing of approximately 1200 nm^{-1} , and a liquid-nitrogen-cooled back-illuminated charge-coupled device (CCD) array having a matrix of $2048 \text{ pixel} \times 512 \text{ pixel}$. The slit width was approximately $600 \mu\text{m}$ and the resolving power was about 350. The Zr filter which is used to block visible light was removed in order to improve the signal. Each spectrum consisted of 10 exposures each lasting 60 s. A bias offset of 7400 counts/column was subtracted from all spectra and spurious signals from cosmic rays were removed. The spectrum counts are the CCD analog-to-digital units (ADU) which result from hardware-binning each column prior to readout to improve the signal-to-noise ratio.

The measured spectra of Rb-like (Dy^{29+}) to Ni-like (Dy^{38+}) ions of dysprosium are shown in Figures 1 and 2. The vertically shifted curves show the second order lines. Well known reference lines of Xe, Ba, Ne, Dy, and O [18,39,40] were used to calibrate the spectra. The observed lines were fitted with a statistically-weighted Gaussian profile. The statistical errors in line positions were less than 0.001 nm. A fourth degree polynomial was used to fit the measured line positions to the known wavelengths. The final wavelength for each line is a weighted average of the wavelengths measured at various beam energies. The quadrature sum of the calibration uncertainty and the statistical uncertainty in fitting the dysprosium line centers results in a final uncertainty of $\sim 0.003 \text{ nm}$.

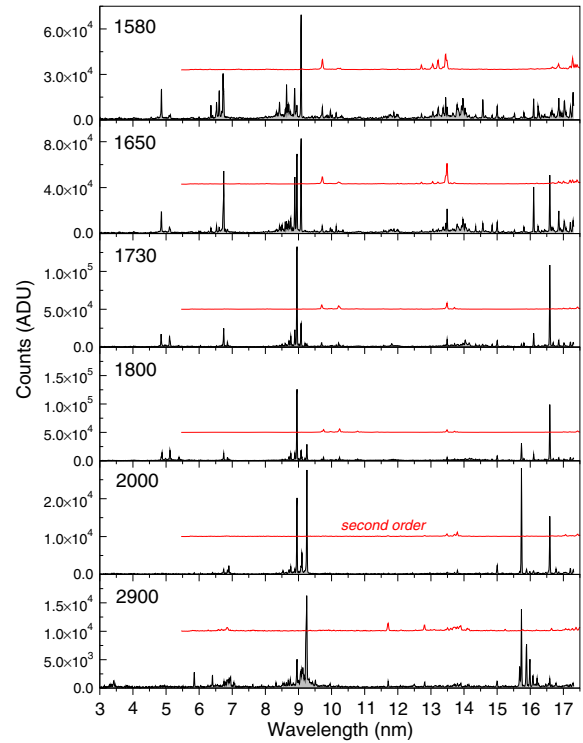


Fig. 2. Experimental spectra of Dy ions. Nominal electron beam energies (in eV) are shown in the upper left corners.

3 Collisional-radiative modeling of Dy spectra

The recorded spectra were compared to simulated spectra produced by modeling the EBIT plasma using the non-Maxwellian collisional-radiative (CR) code NOMAD [41]. This code uses atomic data generated with the Flexible Atomic Code (FAC) [42] including energy levels, rates of radiative decay, electron-impact (de)excitation, ionization, and radiative recombination cross sections. Charge exchange recombination with the background neutral atoms was included as a free parameter. About eight ion stages were typically included in each simulation, with the electron density taken to be $N_e = 10^{12} \text{ cm}^{-3}$. The calculated ionization energies for the dysprosium ions agree with the NIST recommended values [40] to within 1 eV.

The calculation of atomic data for a specific ion was performed in two steps as described in detail in previous works [33,34,43]. First, the relevant atomic data was calculated for all singly-excited (up to $n = 6, 7$, or 8, depending on ion complexity) and some doubly excited configurations. Second, an energy level calculation was performed adding all excitations within the $n = 4$ complex. The energy levels of the lowest configurations were then updated in the CR simulation with these new values. The resulting wavelengths of the simulated spectra agreed much better with the experimental spectra, while the intensities were unaffected. The calculated spectral lines were broadened with a Gaussian instrumental profile and convolved with the spectrometer efficiency curve.

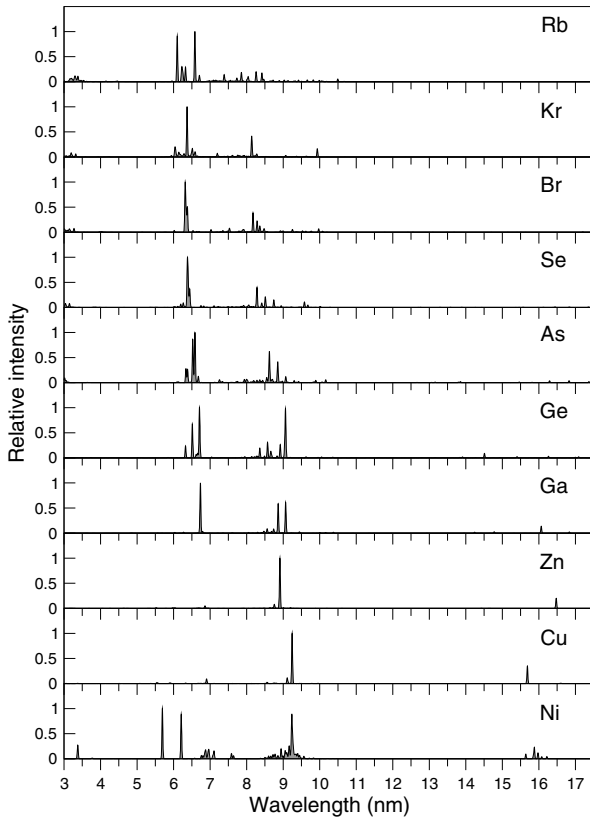


Fig. 3. Simulated normalized spectra based on the CR code NOMAD for the $n = 4-n = 4$ transitions in dysprosium ions. Each charge state is indicated by its isoelectronic sequence.

Identification of spectral lines was achieved by comparing calculated line positions and intensities with spectra measured at several electron beam energies. The simulated Rb-like to Cu-like spectra are presented in Figure 3. One can notice two groups of lines: one near 6.5 nm, the position of which is almost independent of the ion charge, and another moving from about 8.5 nm for Kr-like ion to above 9.2 nm for the Cu-like ion. The shorter-wavelength lines are primarily due to $4p_{1/2}-4d_{3/2}$ electron jumps, for instance, the $4p^6 \ ^1S_0-4p^5 4d \ (1/2, 3/2)_1$ line at ≈ 6.4 nm in the Kr-like ion. The Zn- and Cu-like ions, without $4p$ electrons in the ground state, do not have strong $4p-4d$ transitions in the low-density plasma of EBITs. The longer-wavelength lines are due to several types of transitions: primarily $4p_{3/2}-4d_{5/2}$ for lower ions and then $4s_{1/2}-4p_{3/2}$ in higher ions (Ga-, Zn- and Cu-like), where the ground configuration has no $4p_{3/2}$ electrons. The presence of two groups of lines is well confirmed by the measured spectra shown in Figures 1 and 2.

Comparison of experimental and calculated spectra is exemplified in Figure 4, where the measurements at 1.65 keV are shown along with calculations at 1.58 keV. The lower energy used in the calculations reflects the effect of space charge on the beam electrons. The relative intensities of the calculated lines agree well with the measurements below 10 nm; however, calculations result in significant underestimate of intensities for longer

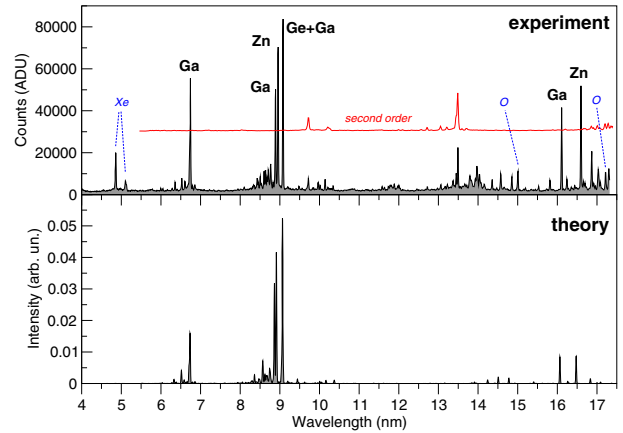


Fig. 4. Comparison of the measured spectrum at 1.65 keV and calculated spectrum at 1.58 keV. The second order spectrum is shifted vertically. Strongest lines are indicated by the corresponding isoelectronic sequences. The Xe and O impurity lines are also indicated in the spectrum.

wavelengths. This may result from uncertainty of the efficiency curve.

4 Line identifications

The strongest line identifications along with current and previous experimental and calculated wavelengths are presented in Table 1. These are given in the jj -coupling scheme as calculated with FAC. Notation l_{\pm} corresponds to the total angular momentum of $j = l \pm 1/2$. The numbers in brackets following the configurations are the assigned energy level number within the ion, where the ground state is level 1 and the first excited state is level 2 and so on. The level identifications show only the largest component of the wave function. In some cases this procedure is not unique due to strong mixing. Consider, for instance, the upper levels 12 and 16 for the 6.728 nm and 6.363 nm lines in the Ge-like ion. For both states the largest component is $4s4p^3 \ ((4s_+, 4p_-)_1, (4p_+^2)_2)_1$ that contributes about 40% and 51% to the wavefunctions of levels 12 and 16, respectively. The next component for both levels is $4s^2 4p_- 4d_-$ at 35% and 38%. A similar strong mixing is observed for levels 37 and 32 in Rb-like ions where the leading component $4p^5 4d^2 \ (4p_-, (4d^2)_2)_{5/2}$ contributes 42% and 40%, whereas the squared expansion coefficients for the next component $4p^6 4f_-$ are 41% and 21%, respectively.

There is good agreement between the present and previously measured wavelengths to within the combined uncertainties. Note that we have included in the calibration the previously identified Zn-like 8.9600 ± 0.0005 nm and 16.5953 ± 0.0005 nm, and Cu-like 9.2603 ± 0.0005 nm and 15.7414 ± 0.0005 nm lines of dysprosium reported in reference [18].

The derived energy levels for ten ions from Dy²⁹⁺ to Dy³⁸⁺ are presented in Table 2. Several levels can only be determined with the aid of calculated values for the lower

Table 1. Wavelengths of spectral lines of highly-charged ions of dysprosium. The uncertainties of other experimental results are given in units of the last significant digit. The FAC level numbers are given in square brackets in the “Conf.” columns. References: a – [18], b – [27], c – [15], d – [25], e – [14], f – [21], g – [16], h – [19], i – [20], j – [13], k – [44], l – [23], m – [22].

| Ion/Seq | Lower level | | Upper level | | λ_{expt} (nm) | | λ_{theor} (nm) | |
|---------|-----------------|----------------------------|---------------------|--|------------------------------|---|-------------------------------|--|
| | Conf. | State | Conf. | State | Current | Previous | Current | Previous |
| 35 [Ga] | $4s^2 4p$ [2] | $(4p_+)_3/2$ | $4s4p^2$ [5] | $((4s_+, 4p_-)_1, 4p_+)_{5/2}$ | 16.864 | | 16.8342 | |
| 33 [As] | $4s^2 4p^3$ [3] | $(4p_-, (4p_+^2)_2)_{5/2}$ | $4s^2 4p^2 4d$ [7] | $(4d_-)_{3/2}$ | 16.837 | | 16.8268 | |
| 36 [Zn] | $4s^2$ [1] | $(4s_+^2)_0$ | $4s4p$ [3] | $(4s_+, 4p_-)_1$ | 16.595 | 16.5953(5) ^a | 16.4753 | 16.6392 ^a , 16.5575 ^b |
| 34 [Ge] | $4s^2 4p^2$ [2] | $(4p_-, 4p_+)_1$ | $4s4p^3$ [6] | $(4s_+, 4p_+)_2$ | 16.243 | | 16.2632 | |
| 38 [Ni] | $3d^9 4s$ [3] | $((3d_+^5)_{5/2}, 4s_+)_2$ | $3d^9 4p$ [6] | $((3d_+^5)_{5/2}, 4p_-)_2$ | 16.212 | | 16.2200 | |
| 35 [Ga] | $4s^2 4p$ [1] | $(4p_-)_{1/2}$ | $4s4p^2$ [3] | $(4s_+)_1/2$ | 16.110 | | 16.0651 | |
| 38 [Ni] | $3d^9 4s$ [5] | $((3d_+^5)_{3/2}, 4s_+)_2$ | $3d^9 4p$ [8] | $((3d_+^5)_{3/2}, 4p_-)_2$ | 16.087 | | 16.0792 | |
| 38 [Ni] | $3d^9 4s$ [3] | $((3d_+^5)_{5/2}, 4s_+)_2$ | $3d^9 4p$ [7] | $((3d_+^5)_{5/2}, 4p_-)_3$ | 15.995 | | 15.9764 | |
| 38 [Ni] | $3d^9 4s$ [2] | $((3d_+^5)_{5/2}, 4s_+)_3$ | $3d^9 4p$ [6] | $((3d_+^5)_{5/2}, 4p_-)_2$ | 15.892 | | 15.8764 | |
| 37 [Cu] | $4s$ [1] | $(4s_+)_1/2$ | $4p$ [2] | $(4p_-)_{1/2}$ | 15.743 | 15.7414(5) ^a | 15.6861 | 15.6889 ^c , 15.741 ^d |
| 38 [Ni] | $3d^9 4s$ [2] | $((3d_+^5)_{5/2}, 4s_+)_3$ | $3d^9 4p$ [7] | $((3d_+^5)_{5/2}, 4p_-)_3$ | 15.689 | | 15.6430 | |
| 34 [Ge] | $4s^2 4p4d$ [9] | $(4p_-, 4d_-)_2$ | $4s^2 4p4d$ [26] | $(4p_+, 4d_+)_2$ | 15.533 | | 15.4030 | |
| 35 [Ga] | $4s^2 4p$ [2] | $(4p_+)_3/2$ | $4s4p^2$ [6] | $((4s_+, 4p_-)_1, 4p_+)_{3/2}$ | 14.856 | | 14.7775 | |
| 34 [Ge] | $4s^2 4p^2$ [3] | $(4p_-, 4p_+)_2$ | $4s4p^3$ [7] | $(4s_+, 4p_+)_1$ | 14.578 | | 14.5103 | |
| 35 [Ga] | $4s^2 4p$ [2] | $(4p_+)_3/2$ | $4s4p^2$ [7] | $((4s_+, 4p_-)_1, 4p_+)_{1/2}$ | 14.362 | | 14.2415 | |
| 29 [Rb] | $4p^6 4d$ [2] | $(4d_+)_5/2$ | $4p^5 4d^2$ [6] | $((4p_+^3)_{3/2}, (4d_+^2)_2)_{7/2}$ | 10.611 | | 10.5643 | |
| 35 [Ga] | $4s^2 4p$ [1] | $(4p_-)_{1/2}$ | $4s4p^2$ [4] | $((4s_+, 4p_-)_0, 4p_+)_{3/2}$ | 10.352 | | 10.3738 | |
| 33 [As] | $4s^2 4p^3$ [1] | $(4p_+)_3/2$ | $4s4p^4$ [6] | $(4s_+, (4p_+^2)_2)_{5/2}$ | 10.142 | | 10.1651 | |
| 31 [Br] | $4p^5$ [1] | $(4p_+^3)_{3/2}$ | $4p^4 4d$ [5] | $((4p_+^2)_2, 4d_-)_{5/2}$ | 10.013 | | 10.013 | |
| 30 [Kr] | $4p^6$ [1] | $(4p_+^4)_0$ | $4p^5 4d$ [3] | $((4p_+^3)_{3/2}, 4d_-)_1$ | 9.962 | | 9.9350 | |
| 33 [As] | $4s^2 4p^3$ [3] | $(4p_-, (4p_+^2)_2)_{5/2}$ | $4s^2 4p^2 4d$ [15] | $((4p_-, 4p_+)_2, 4d_-)_{7/2}$ | 9.900 | | 9.8925 | |
| 32 [Se] | $4s^2 4p^4$ [1] | $(4p_+^2)_2$ | $4p^3 4d$ [8] | $(4p_+, 4d_-)_2$ | 9.758 | | 9.7532 | |
| 32 [Se] | $4s^2 4p^4$ [1] | $(4p_+^2)_2$ | $4p^3 4d$ [10] | $(4p_+, 4d_-)_3$ | 9.706 | | 9.6906 | |
| 37 [Cu] | $4s$ [1] | $(4s_+)_1/2$ | $4p$ [3] | $(4p_+)_{3/2}$ | 9.261 | 9.2603(5) ^a , 9.261(3) ^c , 9.2652(15) ^e | 9.2453 | 9.2538 ^c , 9.260 ^d , 9.237 ^f |
| 36 [Zn] | $4s4p$ [3] | $(4s_+, 4p_-)_1$ | $4p^2$ [8] | $(4p_-, 4p_+)_2$ | 9.206 | | 9.2003 | |
| 37 [Cu] | $4p$ [3] | $(4p_+)_3/2$ | $4d$ [5] | $(4d_+)_5/2$ | 9.112 | 9.1162(15) ^e | 9.1097 | 9.1045 ^g |
| 35 [Ga] | $4s^2 4p$ [1] | $(4p_-)_{1/2}$ | $4s4p^2$ [6] | $((4s_+, 4p_-)_1, 4p_+)_{3/2}$ | 9.084 | 9.090(20) ^f , 8.910(1) ^h | 9.0683 | 8.950 ^f , 8.771 ^h |
| 34 [Ge] | $4s^2 4p^2$ [1] | $(4p_-)_0$ | $4s4p^3$ [7] | $(4s_+, 4p_+)_1$ | 9.085 | | 9.0642 | |
| 36 [Zn] | $4s^2$ [1] | $(4s_+^2)_0$ | $4s4p$ [5] | $(4s_+, 4p_+)_1$ | 8.961 | 8.9600(5) ^a , 8.9591(10) ⁱ , 8.965(2) ^j , 8.9606(20) ^b | 8.9111 | 8.9280 ^a , 8.902 ^f , 8.913 ^j , 8.9032 ^b |
| 35 [Ga] | $4s^2 4p$ [1] | $(4p_-)_{1/2}$ | $4s4p^2$ [7] | $((4s_+, 4p_-)_1, 4p_+)_{1/2}$ | 8.895 | | 8.8636 | |
| 33 [As] | $4s^2 4p^3$ [1] | $(4p_+)_3/2$ | $4s4p^4$ [9] | $(4s_+, (4p_+^2)_2)_{3/2}$ | 8.883 | | 8.8505 | |
| 32 [Se] | $4s^2 4p^4$ [1] | $(4p_+^2)_2$ | $4s4p^5$ [12] | $(4s_+, (4p_+^3)_{3/2})_1$ | 8.812 | | 8.7809 | |
| 36 [Zn] | $4s4p$ [5] | $(4s_+, 4p_+)_1$ | $4s4d$ [14] | $(4s_+, 4d_+)_2$ | 8.777 | | 8.7580 | |
| 33 [As] | $4s^2 4p^3$ [1] | $(4p_+)_3/2$ | $4s^2 4p^2 4d$ [10] | $(4d_+)_5/2$ | 8.648 | | 8.6238 | |
| 35 [Ga] | $4s^2 4p$ [2] | $(4p_+)_3/2$ | $4s4p^2$ [11] | $(4s_+, (4p_+^2)_2)_{3/2}$ | 8.607 | | 8.5624 | |
| 32 [Se] | $4s^2 4p^4$ [1] | $(4p_+^2)_2$ | $4s^2 4p^3 4d$ [13] | $(4p_+, 4d_+)_2$ | 8.612 | | 8.5820 | |
| 32 [Se] | $4s^2 4p^4$ [2] | $(4p_+^2)_0$ | $4s^2 4p^3 4d$ [15] | $(4p_+, 4d_+)_1$ | 8.528 | | 8.4915 | |
| 29 [Rb] | $4p^6 4d$ [1] | $(4d_-)_{3/2}$ | $4p^5 4d^2$ [23] | $((4p_+^3)_{3/2}, 4d_-)_2, 4d_+)_5/2$ | 8.500 | | 8.4526 | |
| 34 [Ge] | $4s^2 4p^2$ [2] | $(4p_-, 4p_+)_1$ | $4s4p^3$ [16] | $((4s_+, 4p_-)_1, (4p_+^2)_2)_1$ | 8.435 | | 8.3603 | |
| 32 [Se] | $4s^2 4p^4$ [1] | $(4p_+^2)_2$ | $4s^2 4p^3 4d$ [14] | $(4p_+, 4d_+)_3$ | 8.412 | | 8.3804 | |
| 31 [Br] | $4p^5$ [1] | $(4p_+^3)_{3/2}$ | $4p^4 4d$ [13] | $((4p_+^2)_2, 4d_+)_3/2$ | 8.399 | | 8.3627 | |
| 29 [Rb] | $4p^6 4d$ [1] | $(4d_-)_{3/2}$ | $4p^5 4d^2$ [25] | $((4p_+^3)_{3/2}, 4d_-)_3, 4d_+)_3/2$ | 8.352 | | 8.3020 | |
| 31 [Br] | $4p^5$ [1] | $(4p_+^3)_{3/2}$ | $4p^4 4d$ [14] | $((4p_+^2)_2, 4d_+)_5/2$ | 8.287 | | 8.2468 | |
| 30 [Kr] | $4p^6$ [1] | $(4p_+^4)_0$ | $4p^5 4d$ [9] | $((4p_+^3)_{3/2}, 4d_+)_1$ | 8.195 | | 8.1385 | |
| 29 [Rb] | $4p^6 4d$ [1] | $(4d_-)_{3/2}$ | $4p^5 4d^2$ [28] | $((4p_+^3)_{3/2}, 4d_-)_3, 4d_+)_1/2$ | 7.959 | | 7.8952 | |
| 29 [Rb] | $4p^6 4d$ [2] | $(4d_+)_5/2$ | $4p^6 4f$ [33] | $(4f_+)_{7/2}$ | 7.801 | | 7.7451 | 7.767 ^k |
| 29 [Rb] | $4p^6 4d$ [1] | $(4d_-)_{3/2}$ | $4p^5 4d^2$ [32] | $(4p_-, (4d_-)_2)_{5/2}$ | 7.449 | | 7.4084 | |
| 37 [Cu] | $4p$ [2] | $(4p_-)_{1/2}$ | $4d$ [4] | $(4d_-)_{3/2}$ | 6.905 | 6.9080(15) ^e | 6.9035 | 6.9037 ^g |
| 29 [Rb] | $4p^6 4d$ [1] | $(4d_-)_{3/2}$ | $4p^5 4d^2$ [38] | $(4p_-, (4d_-)_2)_{5/2}$ | 6.803 | | 6.6802 | |
| 35 [Ga] | $4s^2 4p$ [1] | $(4p_-)_{1/2}$ | $4s^2 4d$ [9] | $(4d_-)_{3/2}$ | 6.750 | 6.750(1) ^h | 6.7343 | 6.674 ^h |
| 34 [Ge] | $4s^2 4p^2$ [1] | $(4p_-)_0$ | $4s4p^3$ [12] | $((4s_+, 4p_-)_1, (4p_+^2)_2)_1$ | 6.728 | | 6.7093 | |
| 33 [As] | $4s^2 4p^3$ [1] | $(4p_+)_3/2$ | $4s^2 4p^2 4d$ [20] | $((4p_-, 4p_+)_1, 4d_+)_5/2$ | 6.613 | | 6.5862 | |
| 34 [Ge] | $4s^2 4p^2$ [1] | $(4p_-)_0$ | $4s4p^3$ [13] | $((4s_+, 4p_-)_1, (4p_+^2)_0)_1$ | 6.534 | | 6.5141 | |
| 32 [Se] | $4s^2 4p^4$ [1] | $(4p_+^2)_2$ | $4s^2 4p^3 4d$ [29] | $((4p_-, (4p_+^2)_2)_{5/2}, 4d_-)_3$ | 6.545 | | 6.5015 | |
| 32 [Se] | $4s^2 4p^4$ [1] | $(4p_+^2)_2$ | $4s^2 4p^3 4d$ [30] | $((4p_-, (4p_+^2)_2)_{3/2}, 4d_-)_2$ | 6.512 | | 6.4670 | |
| 31 [Br] | $4p^5$ [1] | $(4p_+^3)_{3/2}$ | $4p^4 4d$ [24] | $((4p_-, (4p_+^3)_{3/2})_2, 4d_-)_1/2$ | 6.517 | | 6.4602 | |
| 31 [Br] | $4p^5$ [1] | $(4p_+^3)_{3/2}$ | $4p^4 4d$ [25] | $((4p_-, (4p_+^3)_{3/2})_2, 4d_-)_3/2$ | 6.497 | | 6.4526 | |
| 31 [Br] | $4p^5$ [1] | $(4p_+^3)_{3/2}$ | $4p^4 4d$ [27] | $((4p_-, (4p_+^3)_{3/2})_2, 4d_-)_5/2$ | 6.457 | | 6.4048 | |
| 30 [Kr] | $4p^6$ [1] | $(4p_+^4)_0$ | $4p^5 4d$ [13] | $(4p_-, 4d_-)_1$ | 6.435 | | 6.3689 | |
| 33 [As] | $4s^2 4p^3$ [1] | $(4p_+)_3/2$ | $4s^2 4p^2 4d$ [22] | $((4p_-, 4p_+)_1, 4d_-)_{3/2}$ | 6.416 | | 6.3834 | |
| 38 [Ni] | $3d^9 4p$ [12] | $((3d_+^5)_{5/2}, 4p_+)_1$ | $3d^9 4d$ [35] | $((3d_+^5)_{3/2}, 4d_-)_0$ | 6.409 | 6.41(2) ^l | 6.2094 | 6.406 ^l , 6.406 ^m |
| 34 [Ge] | $4s^2 4p^2$ [1] | $(4p_-)_0$ | $4s4p^3$ [16] | $((4s_+, 4p_-)_1, (4p_+^2)_2)_1$ | 6.363 | | 6.3273 | |
| 29 [Rb] | $4p^6 4d$ [1] | $(4d_-)_{3/2}$ | $4p^5 4d^2$ [45] | $(4p_-, (4d_-)_2)_{3/2}$ | 6.271 | | 6.2163 | 6.147 ^k |
| 38 [Ni] | $3d^9 4p$ [9] | $((3d_+^5)_{3/2}, 4p_-)_1$ | $3d^9 4d$ [35] | $((3d_+^5)_{3/2}, 4d_-)_0$ | 5.858 | 5.85(2) ^l | 5.6931 | 5.856 ^l , 5.857 ^m |

Table 2. Energy levels of highly-charged ions of dysprosium.

| Ion/Seq | Conf. | State | J | Level No. (FAC) | Energy (cm ⁻¹) | Unc. (cm ⁻¹) |
|---------|------------------------------------|---|-----|-----------------|----------------------------|--------------------------|
| 29 [Rb] | 4p ⁶ 4d | 4d ₋ | 3/2 | 1 | 0 | |
| 29 [Rb] | 4p ⁶ 4d | 4d ₊ | 5/2 | 2 | 80 600 + x | FAC |
| 29 [Rb] | 4p ⁵ 4d ² | (4p ₋ , (4d ²) ₂) | 5/2 | 6 | 1 023 000 + x | 300 |
| 29 [Rb] | 4p ⁵ 4d ² | ((4p ₊ ³) _{3/2} , 4d ₋) ₃ , 4d ₊ | 5/2 | 23 | 1 176 500 | 400 |
| 29 [Rb] | 4p ⁵ 4d ² | ((4p ₊ ³) _{3/2} , 4d ₋) ₃ , 4d ₊ | 3/2 | 25 | 1 197 300 | 400 |
| 29 [Rb] | 4p ⁵ 4d ² | ((4p ₊ ³) _{3/2} , 4d ₋) ₃ , 4d ₊ | 1/2 | 28 | 1 256 400 | 500 |
| 29 [Rb] | 4p ⁵ 4d ² | (4p ₋ , (4d ²) ₂) | 5/2 | 32 | 1 342 500 | 500 |
| 29 [Rb] | 4p ⁶ 4f | 4f ₊ | 7/2 | 33 | 1 362 500 + x | 500 |
| 29 [Rb] | 4p ⁵ 4d ² | (4p ₋ , (4d ²) ₂) | 5/2 | 38 | 1 469 900 | 600 |
| 29 [Rb] | 4p ⁵ 4d ² | (4p ₋ , (4d ²) ₂) | 3/2 | 45 | 1 594 600 | 700 |
| 30 [Kr] | 4p ⁶ | 4p ₊ ⁴ | 0 | 1 | 0 | |
| 30 [Kr] | 4p ⁵ 4d | ((4p ₊ ³) _{3/2} , 4d ₋) | 1 | 3 | 1 003 800 | 300 |
| 30 [Kr] | 4p ⁵ 4d | ((4p ₊ ³) _{3/2} , 4d ₊) | 1 | 9 | 1 220 300 | 400 |
| 30 [Kr] | 4p ⁵ 4d | (4p ₋ , 4d ₋) | 1 | 13 | 1 554 000 | 700 |
| 31 [Br] | 4p ⁵ | 4p ₊ ³ | 3/2 | 1 | 0 | |
| 31 [Br] | 4p ⁴ 4d | ((4p ₊ ²) ₂ , 4d ₋) | 5/2 | 5 | 998 700 | 300 |
| 31 [Br] | 4p ⁴ 4d | ((4p ₊ ²) ₂ , 4d ₊) | 3/2 | 13 | 1 190 600 | 400 |
| 31 [Br] | 4p ⁴ 4d | ((4p ₊ ²) ₂ , 4d ₊) | 5/2 | 14 | 1 206 700 | 400 |
| 31 [Br] | 4p ⁴ 4d | ((4p ₋ , (4p ₊ ³) _{3/2}) ₂ , 4d ₋) | 1/2 | 24 | 1 534 400 | 700 |
| 31 [Br] | 4p ⁴ 4d | ((4p ₋ , (4p ₊ ³) _{3/2}) ₂ , 4d ₋) | 3/2 | 25 | 1 539 200 | 700 |
| 31 [Br] | 4p ⁴ 4d | ((4p ₋ , (4p ₊ ³) _{3/2}) ₂ , 4d ₋) | 5/2 | 27 | 1 548 700 | 700 |
| 32 [Se] | 4s ² 4p ⁴ | 4p ₊ ² | 2 | 1 | 0 | |
| 32 [Se] | 4s ² 4p ⁴ | 4p ₊ ² | 0 | 2 | 60 060 + x | FAC |
| 32 [Se] | 4s ² 4p ³ 4d | (4p ₊ , 4d ₋) | 2 | 8 | 1 024 800 | 300 |
| 32 [Se] | 4s ² 4p ³ 4d | (4p ₊ , 4d ₋) | 3 | 10 | 1 030 300 | 300 |
| 32 [Se] | 4s4p ⁵ | (4s ₊ , (4p ₊ ³) _{3/2}) | 1 | 12 | 1 134 800 | 400 |
| 32 [Se] | 4s ² 4p ³ 4d | (4p ₊ , 4d ₊) | 2 | 13 | 1 161 200 | 400 |
| 32 [Se] | 4s ² 4p ³ 4d | (4p ₊ , 4d ₊) | 3 | 14 | 1 188 800 | 400 |
| 32 [Se] | 4s ² 4p ³ 4d | (4p ₊ , 4d ₊) | 1 | 15 | 1 232 700 + x | 400 |
| 32 [Se] | 4s ² 4p ³ 4d | ((4p ₋ , (4p ₊ ²) ₂) _{5/2} , 4d ₋) | 3 | 29 | 1 527 900 | 700 |
| 32 [Se] | 4s ² 4p ³ 4d | ((4p ₋ , (4p ₊ ²) ₂) _{3/2} , 4d ₋) | 2 | 30 | 1 535 600 | 700 |
| 33 [As] | 4s ² 4p ³ | 4p ₊ | 3/2 | 1 | 0 | |
| 33 [As] | 4s ² 4p ³ | (4p ₋ , (4p ₊ ²) ₂) | 5/2 | 3 | 480 070 + x | FAC |
| 33 [As] | 4s4p ⁴ | (4s ₊ , (4p ₊ ²) ₂) | 5/2 | 6 | 986 000 | 300 |
| 33 [As] | 4s ² 4p ² 4d | 4d ₋ | 3/2 | 7 | 1 074 000 + x | 200 |
| 33 [As] | 4s4p ⁴ | (4s ₊ , (4p ₊ ²) ₂) | 3/2 | 9 | 1 125 700 | 400 |
| 33 [As] | 4s ² 4p ² 4d | 4d ₊ | 5/2 | 10 | 1 156 300 | 400 |
| 33 [As] | 4s ² 4p ² 4d | ((4p ₋ , 4p ₊) ₂ , 4d ₋) | 7/2 | 15 | 1 490 200 + x | 450 |
| 33 [As] | 4s ² 4p ² 4d | ((4p ₋ , 4p ₊) ₁ , 4d ₊) | 5/2 | 20 | 1 512 200 | 700 |
| 33 [As] | 4s ² 4p ² 4d | ((4p ₋ , 4p ₊) ₁ , 4d ₋) | 3/2 | 22 | 1 558 600 | 700 |
| 34 [Ge] | 4s ² 4p ² | 4p ₋ ² | 0 | 1 | 0 | |
| 34 [Ge] | 4s ² 4p ² | (4p ₋ , 4p ₊) | 1 | 2 | 386 100 | 220 |
| 34 [Ge] | 4s ² 4p ² | (4p ₋ , 4p ₊) | 2 | 3 | 414 700 | 160 |
| 34 [Ge] | 4s4p ³ | (4s ₊ , 4p ₊) | 2 | 6 | 1 001 750 | 600 |
| 34 [Ge] | 4s4p ³ | (4s ₊ , 4p ₊) | 1 | 7 | 1 100 700 | 400 |
| 34 [Ge] | 4s ² 4p4d | (4p ₋ , 4d ₋) | 2 | 9 | 1 388 800 + x | FAC |
| 34 [Ge] | 4s4p ³ | ((4s ₊ , 4p ₋) ₁ , (4p ₊ ²) ₂) | 1 | 12 | 1 486 300 | 700 |
| 34 [Ge] | 4s4p ³ | ((4s ₊ , 4p ₋) ₁ , (4p ₊ ²) ₀) | 1 | 13 | 1 530 500 | 700 |
| 34 [Ge] | 4s4p ³ | ((4s ₊ , 4p ₋) ₁ , (4p ₊ ²) ₂) | 1 | 16 | 1 571 600 | 700 |
| 34 [Ge] | 4s ² 4p4d | (4p ₊ , 4d ₊) | 2 | 26 | 2 032 600 + x | 400 |
| 35 [Ga] | 4s ² 4p | 4p ₋ | 1/2 | 1 | 0 | |
| 35 [Ga] | 4s ² 4p | 4p ₊ | 3/2 | 2 | 427 800 | 300 |
| 35 [Ga] | 4s4p ² | 4s ₊ | 1/2 | 3 | 620 700 | 120 |
| 35 [Ga] | 4s4p ² | ((4s ₊ , 4p ₋) ₀ , 4p ₊) | 3/2 | 4 | 966 000 | 300 |
| 35 [Ga] | 4s4p ² | ((4s ₊ , 4p ₋) ₀ , 4p ₊) | 5/2 | 5 | 1 020 900 | 400 |
| 35 [Ga] | 4s4p ² | ((4s ₊ , 4p ₋) ₁ , 4p ₊) | 3/2 | 6 | 1 100 800 | 400 |

Table 2. Continued.

| Ion/Seq | Conf. | State | J | Level No. (FAC) | Energy (cm ⁻¹) | Unc. (cm ⁻¹) |
|---------|--------------------|--|-----|-----------------|----------------------------|--------------------------|
| 35 [Ga] | 4s4p ² | ((4s ₊ ,4p ₋) ₁ ,4p ₊) | 1/2 | 7 | 1 124 200 | 400 |
| 35 [Ga] | 4s ² 4d | 4d ₋ | 3/2 | 9 | 1 481 500 | 700 |
| 35 [Ga] | 4s4p ² | (4s ₊ ,(4p ₊) ₂) | 3/2 | 11 | 1 589 700 | 840 |
| 36 [Zn] | 4s ² | 4s ₊ ² | 0 | 1 | 0 | |
| 36 [Zn] | 4s4p | (4s ₊ ,4p ₋) | 1 | 3 | 602 600 | 110 |
| 36 [Zn] | 4s4p | (4s ₊ ,4p ₊) | 1 | 5 | 1 115 900 | 400 |
| 36 [Zn] | 4p ² | (4p ₋ ,4p ₊) | 2 | 8 | 1 688 800 | 600 |
| 36 [Zn] | 4s4d | (4s ₊ ,4d ₊) | 2 | 14 | 2 255 200 | 1100 |
| 37 [Cu] | 4s | 4s ₊ | 1/2 | 1 | 0 | |
| 37 [Cu] | 4p | 4p ₋ | 1/2 | 2 | 635 200 | 120 |
| 37 [Cu] | 4p | 4p ₊ | 3/2 | 3 | 1 079 800 | 350 |
| 37 [Cu] | 4d | 4d ₋ | 3/2 | 4 | 2 083 400 | 1000 |
| 37 [Cu] | 4d | 4d ₊ | 5/2 | 5 | 2 177 300 | 1000 |
| 38 [Ni] | 3d ¹⁰ | 3d ₊ ⁶ | 0 | 1 | 0 | |
| 38 [Ni] | 3d ⁹ 4s | ((3d ₊ ⁵) _{5/2} ,4s ₊) | 3 | 2 | 9 099 290 + x | Ref. [45] |
| 38 [Ni] | 3d ⁹ 4s | ((3d ₊ ⁵) _{5/2} ,4s ₊) | 2 | 3 | 9 111 600 + x | 170 |
| 38 [Ni] | 3d ⁹ 4s | ((3d ₋ ³) _{3/2} ,4s ₊) | 2 | 5 | 9 413 650 + y | Ref. [45] |
| 38 [Ni] | 3d ⁹ 4p | ((3d ₊ ⁵) _{5/2} ,4p ₋) | 2 | 6 | 9 728 500 + x | 120 |
| 38 [Ni] | 3d ⁹ 4p | ((3d ₊ ⁵) _{5/2} ,4p ₋) | 3 | 7 | 9 736 700 + x | 150 |
| 38 [Ni] | 3d ⁹ 4p | ((3d ₋ ³) _{3/2} ,4p ₋) | 2 | 8 | 10 035 300 + y | 120 |
| 38 [Ni] | 3d ⁹ 4p | ((3d ₋ ³) _{3/2} ,4p ₋) | 1 | 9 | 10 058 300 + z | Ref. [45] |
| 38 [Ni] | 3d ⁹ 4p | ((3d ₊ ⁵) _{5/2} ,4p ₊) | 1 | 12 | 10 205 000 + z | 1100 |
| 38 [Ni] | 3d ⁹ 4d | ((3d ₋ ³) _{3/2} ,4d ₋) | 0 | 35 | 11 765 300 + z | 900 |

level of a transition. Since the lower level is not known experimentally in these cases, the energies are given with a “+x”. In most cases the reference energies were calculated with FAC; however, for the Ni-like ion we made use of the more accurate energies calculated with the relativistic many-body perturbation theory (RMBPT) [45].

The experimental spectra were used to confirm identification of some newly identified lines using the Ritz energies. Using the Ni-like ion as an example, the lines 15.689 nm, 15.892 nm, 15.995 nm and 16.212 nm, connect levels 2 and 3 with level 6 and level 7 (see Tab. 2). It is obvious that the energy difference between levels 2 and 3 calculated from the differences of wavenumbers for two pairs of transitions should be the same. Indeed, the 2-6 and 3-6 lines give $\Delta E_{\text{Ni}}(2-3) = (12\,420 \pm 170) \text{ cm}^{-1}$, and the 2-7 and 3-7 transitions result in a close value of $(12\,190 \pm 170) \text{ cm}^{-1}$. A similar analysis for the spectral lines connecting levels 1 and 2 with levels 6, and 7 in the Ga-like ion also confirms our identifications. Our measured value of $\Delta E_{\text{Ga}}(1-2)$ is $(427\,800 \pm 300) \text{ cm}^{-1}$. The semiempirical result of $427\,670 \text{ cm}^{-1}$ [46] and the RMBPT value of $428\,015 \text{ cm}^{-1}$ [47] both agree well with our result. However, the MCDF energy of $426\,675 \text{ cm}^{-1}$ [48] significantly differs from the measurement.

5 Conclusion

EUV spectra from highly charged ions of dysprosium were recorded at the NIST EBIT. Forty nine new lines were identified in Rb-like to Ni-like ions. Several strongest lines

lie in the 6.6 nm to 6.8 nm wavelength region proposed for next generation lithography. Of note is the strongly emitting Rb-like dysprosium line at 6.803 nm which could be coupled with highly reflective LaN/B₄C multilayer mirrors. An alternative EUV source could be based on a similar Rb-like gadolinium line which was previously found to emit strongly at 6.827 nm. These transitions could be optimized in a laser-produced plasma source for future next generation EUV lithography.

This work was supported by Science Foundation Ireland under Principal Investigator research Grant 07/IN.1/I1771 and in part by the Office of Fusion Energy Sciences of the US Department of Energy. We are grateful to U.I. Safronova for providing the RMBPT energies from reference [45].

References

1. S.S. Churilov, R.R. Kildiyarova, A.N. Ryabtsev, S.V. Sadovsky, Phys. Scr. **80**, 045303 (2009)
2. T. Otsuka, D. Kilbane, T. Higashiguchi, N. Yugami, T. Yatagai, W. Jiang, A. Endo, P. Dunne, G. O’Sullivan, Appl. Phys. Lett. **97**, 111503 (2010)
3. T. Otsuka, D. Kilbane, T. Higashiguchi, N. Yugami, T. Yatagai, W. Jiang, A. Endo, P. Dunne, G. O’Sullivan, Appl. Phys. Lett. **97**, 231503 (2010)
4. D. Kilbane, G. O’Sullivan, J. Appl. Phys. **108**, 104905 (2010)
5. A. Sasaki, K. Nishihara, A. Sunahara, H. Furukawa, T. Nishikawa, F. Koike, Appl. Phys. Lett. **97**, 231501 (2010)

6. M. Masnavi, J. Szilagy, H. Parchamy, M.C. Richardson, *Appl. Phys. Lett.* **102**, 164102 (2013)
7. G. O'Sullivan, P.K. Carroll, *J. Opt. Soc. Am.* **71**, 227 (1981)
8. P.K. Carroll, G. O'Sullivan, *Phys. Rev. A* **25**, 275 (1982)
9. D. Kilbane, G. O'Sullivan, *Phys. Rev. A* **82**, 062504 (2010)
10. D. Kilbane, *J. Phys. B* **44**, 165006 (2011)
11. I.A. Makhotkin, E. Zoethout, E. Louis, A.M. Yakunin, S. Müllender, F. Bijkerk, *J. Micro/Nanolith. MEMS MOEMS* **11**, 040501 (2012)
12. R. Soufli, A.L. Aquila, F. Salmassi, M. Fernández-Perea, E.M. Gullikson, *Appl. Opt.* **47**, 4633 (2008)
13. J. Reader, G. Luther, *Phys. Rev. Lett.* **45**, 609 (1980)
14. J. Reader, G. Luther, *Phys. Scr.* **24**, 732 (1981)
15. J.F. Seely, U. Feldman, A.W. Wouters, J.L. Schwob, S. Suckewer, *Phys. Rev. A* **40**, 5020 (1989)
16. J.F. Seely, C.M. Brown, U. Feldman, *At. Data Nucl. Data Tables* **43**, 145 (1989)
17. M. Finkenthal, S. Lippmann, L.K. Huang, H.W. Moos, Y.T. Lee, N. Spector, A. Zigler, E. Yarkoni, *Phys. Scr.* **41**, 445 (1990)
18. J. Sugar, V. Kaufman, D.H. Baik, Y.K. Kim, W.L. Rowan, *J. Opt. Soc. Am. B* **8**, 1795 (1991)
19. K.B. Fournier, W.H. Goldstein, A. Osterheld, M. Finkenthal, S. Lippmann, L.K. Huang, H.W. Moos, N. Spector, *Phys. Rev. A* **50**, 2248 (1994)
20. N. Acquista, J. Reader, *J. Opt. Soc. Am. B* **1**, 649 (1984)
21. P. Mandelbaum, M. Finkenthal, E. Meroz, J.L. Schwob, J. Oreg, W.H. Goldstein, M.K.L. Osterheld, A.B. Shalom, S. Lippman, L.K. Huang, H.W. Moos, *Phys. Rev. A* **42**, 4412 (1990)
22. J.H. Scofield, B.J. MacGowan, *Phys. Scr.* **46**, 361 (1992)
23. H. Daido, S. Ninomiya, M. Takagi, Y. Kato, *J. Opt. Soc. Am. B* **16**, 296 (1999)
24. I.P. Grant, B.J. McKenzie, P.H. Norrington, D.F. Mayers, N.C. Pyper, *Comput. Phys. Commun.* **21**, 207 (1980)
25. Y.K. Kim, D.H. Baik, P. Indelicato, J.P. Desclaux, *Phys. Rev. A* **44**, 148 (1991)
26. J.P. Desclaux, *Comput. Phys. Commun.* **9**, 31 (1975)
27. C.M. Brown, J.F. Seely, D.R. Kania, B.A. Hammel, C.A. Back, R.W. Lee, A. Bar-Shalom, W.E. Behring, *At. Data Nucl. Data Tables* **58**, 203 (1994)
28. A. Bar-Shalom, M. Klapisch, J. Oreg, *J. Quant. Spectrosc. Radiat. Transfer* **71**, 169 (2001)
29. M. Klapisch, *Comput. Phys. Commun.* **2**, 269 (1971)
30. M. Klapisch, J.L. Schwob, B.S. Fraenkel, J. Oreg, *J. Opt. Soc. Am.* **67**, 148 (1977)
31. K.G. Dylla, I.P. Grant, C.T. Johnson, F.A. Parpia, E.P. Plummer, *Comput. Phys. Commun.* **55**, 425 (1988)
32. Yu. Ralchenko, J. Reader, J.M. Pomeroy, J.N. Tan, J.D. Gillasp, *J. Phys. B* **40**, 3861 (2007)
33. I. Draganić, Yu. Ralchenko, J. Reader, J.D. Gillasp, J.N. Tan, J.M. Pomeroy, S.M. Brewer, D. Osin, *J. Phys. B* **44**, 025001 (2011)
34. D. Kilbane, G. O'Sullivan, J.D. Gillasp, Yu. Ralchenko, J. Reader, *Phys. Rev. A* **86**, 042503 (2012)
35. D. Kilbane, J.D. Gillasp, Yu. Ralchenko, J. Reader, G. O'Sullivan, *Phys. Scr.* **T156**, 014012 (2013)
36. J.D. Gillasp, *Phys. Scr.* **T71**, 99 (1997)
37. G.E. Holland, C.N. Boyer, J.F. Seely, J.N. Tan, J.M. Pomeroy, J.D. Gillasp, *Rev. Sci. Instrum.* **76**, 073304 (2005)
38. B. Blagojević, E.O.L. Bigot, K. Fahy, A. Aguilar, K. Makonyi, E. Takács, J.N. Tan, J.M. Pomeroy, J.H. Burnett, J.D. Gillasp, J.R. Roberts, *Rev. Sci. Instrum.* **76**, 083102 (2005)
39. D. Osin, J. Reader, J.D. Gillasp, Yu. Ralchenko, *J. Phys. B* **45**, 245001 (2012)
40. A. Kramida, Yu. Ralchenko, J. Reader, NIST ASD Team, *NIST Atomic Spectra Database (ver. 5.1)* (National Institute of Standards and Technology, Gaithersburg, MD, 2013), <http://physics.nist.gov/asd>
41. Yu.V. Ralchenko, Y. Maron, *J. Quant. Spectrosc. Radiat. Transfer* **71**, 609 (2001)
42. M.F. Gu, *Can. J. Phys.* **86**, 675 (2008)
43. Yu. Ralchenko, I.N. Draganić, D. Osin, J.D. Gillasp, J. Reader, *Phys. Rev. A* **83**, 032517 (2011)
44. M. Finkenthal, A.S. Lippmann, L.K. Huang, T.L. Yu, B.C. Stratton, H.W. Moos, M. Klapisch, P. Mandelbaum, A.B. Shalom, W.L. Hodge, P.E. Phillips, T.R. Price, J.C. Porter, B. Richards, W.L. Rowan, *J. Appl. Phys.* **59**, 3644 (1986)
45. U.I. Safronova, A.S. Safronova, P. Beiersdorfer, *J. Phys. B* **40**, 955 (2007)
46. L.J. Curtis, *Phys. Rev. A* **35**, 2089 (1987)
47. U.I. Safronova, T.E. Cowan, M.S. Safronova, *Phys. Lett. A* **348**, 293 (2006)
48. M.A. Ali, *Phys. Scr.* **55**, 159 (1997)